Journal of Chemical and Petroleum Engineering 2020, 54(1): 13-33
DOI: 10.22059/jchpe.2019.280824.1277

RESEARCH PAPER

Low-Temperature Catalytic Cracking of Heavy Feedstock Optimized by Response Surface Method

Sina Alizad[a], Elham Sadat Moosavi[b], Ramin Karimzadeh[a,*]

a. Chemical Engineering Faculty, Tarbiat Modares University, Tehran, Tehran, P.O. Box 14155-4838, Iran
b. Department of Materials and Chemical Engineering, Buein Zahra Technical University, Buein Zahra, Qazvin, P.O. Box 34517-45346, Iran

Received: 7 May 2019, Revised: 23 October 2019, Accepted: 4 December 2019

Abstract

Upgrading of cracked PFO (Pyrolysis fuel oil) for the production of liquid fuels, such as gasoline and light gasoil, was carried out in a semi-batch reactor. Two different kinds of mesoporous and microporous catalysts, MCM-41 and ZSM-5, were used. Modification methods, such as ion exchange and impregnation with Fe and Ti, were done for tuning the acidity of the catalyst. XRD, FT-IR, and XRF analyzes were used to identify the structure and composition of the catalysts. Among the catalysts used in low-temperature catalytic cracking of cracked PFO at a moderate temperature (380 °C), 3%Ti/H-MCM-41 showed the best catalytic performance. After choosing the best catalyst, an experimental design was carried out using a response surface method with a five-level central composite design model. The effect of 3 main parameters, i.e. reaction temperature (360-400 °C), catalyst to feed ratio (0.04-0.1), and loading of Ti (0-5%) was investigated on liquid productivity and light olefin production. Design Expert software was used to maximize the sum of liquid yield and olefins in the gas. In optimum condition (380 °C) with the ratio of 0.1 g/g catalyst to feed over 2.5%Ti/H-MCM-41, the wt. % of liquid, gas, and solid products are 80 wt. %, 10 wt. %, and 10 wt. %, respectively. At this condition, 26 wt. % of liquid product was in the range of gasoline (C5-C10) and the rest (i.e. C11+) was considered in the range of light gas oil. Light olefins of the obtained gas products were about 2.74 wt. %.

Keywords:
Al-MCM-41,
Catalytic Cracking,
Pyrolysis Fuel Oil,
Response Surface,
ZSM-5

Introduction

The decreasing trend of light crude oil supply and increasing demand for liquid fuels in developing countries, encourage researchers to provide new methods of conversion of heavy feedstock such as atmospheric residue, to light ones [1,2], vacuum residue[3-6], and vacuum gas oil[7-10], or wastes [11,12], to light liquid fuels. Various methods of cracking, such as thermal cracking [13,14], catalytic cracking [15-17], and hydrocatalytic cracking [18,19], are used to produce high-value products, such as gasoline. Thermal cracking is the oldest method of cracking which is no more a suitable method because of being energy-intensive and expensive. Therefore, in order to decrease the temperature of degradation, researchers introduced catalytic cracking and hydrocatalytic cracking. In refinery and petrochemical companies, the capital and operating cost of hydrogen production units are very high, so catalytic cracking is a unique method to convert low-value heavy feedstocks to high-value fuels. Energy consumption in oil industries is so important that researchers are very eager to reduce

* Corresponding author:
Email: ramin@modares.ac.ir (R. Karimzadeh).

the catalytic reaction temperature to save money and reduce the emission of carbon dioxide to the air. The temperature of catalytic cracking varies between 350 °C and 650 °C [20], but some researchers introduced a unique method to perform the reaction at the lowest possible temperature [21].

Different types of heterogeneous catalysts such as metal [3], alumina, silica, and aluminosilicate materials [22,23], were used in catalytic cracking of heavy feedstocks. Metal catalysts have a high conversion rate in chemical reactions, but using this type of catalysts raises the capital cost significantly. Researchers are very interested in catalytic cracking of heavy feedstock using porous catalysts such as alumina, silica, and aluminosilicate materials because of their high surface area, low cost of production, and availability. Among the porous catalysts, aluminosilicate materials, such as ZSM-5 [24-26], Y [4,27], and MCM-41[21,26] zeolites showed high catalytic activity in comparison with others. ZSM-5 zeolite is an appropriate selective catalyst for the production of light olefins because of having the mesoporous structure that is suitable for the diffusion of small molecules. MCM-41 zeolite is a suitable catalyst for the diffusion of large molecules of heavy hydrocarbon feedstock in the production of liquid fuels because of its mesoporous structure.

Many different methods of modification were introduced to tune the acidity of catalyst and increase the catalytic activity of zeolites. Ion exchange is a very common method to form an acidic form of zeolites using ammonium nitrate or ammonium chloride. Ion exchange increases the acidity of catalyst, as a result of which catalyst activity increases, too. Adding the active metal sites to the surface of zeolite catalysts is another method of modification that increases the catalyst activity in reaction and helps to tune of the acidity. Loading of different metals such as Ti [28-33], Fe [34,35], La [36], and many other metals [37], with varying amount of 0.1-20 wt. % were investigated in previous researches. When the loading amount is more than 12 wt. % clusters of the metal is formed on the surface of the zeolites, so small amount of the loading is recommended to form a uniform surface of the modified catalyst. Also, a higher amount of loading blocks the caves of the catalyst and reduces the surface area which leads to decreased catalyst activity. Among all metals, Ti and Fe have the best performance in catalytic reaction for producing light olefin.

In this research, we used a unique method with a simple reaction set up to produce gasoline and gas oil in a minimum temperature of catalytic cracking of a low-value heavy feedstock. Thermal cracking is very energy-intensive and in hydro catalytic cracking method, hydrogen production units increase the capital and operating costs. Catalytic cracking is more suitable if the temperature of catalytic cracking decreased to the minimum effective temperature. In refinery and petrochemical industries continuous reactors used generally, but in this work for studying the applicability of low-temperature catalytic cracking, we used a semi-batch reactor. The feedstock which is used in this study is different from common heavy feedstocks such as atmospheric residue, vacuum residue, and vacuum gas oil obtained from the refinery. Here, the feedstock, obtained from a petrochemical company, includes a high amount of aromatic which is hardly cracked and the cracking of this type of heavy feedstock was not previously performed. Also, the response surface method is used to determine the desired value of the 3 key parameters of catalytic cracking to maximize high-quality liquid fuel production. Finding the best operating condition for the parameters of the temperature of catalytic cracking, catalyst to feed ratio, and percent of Ti loading is the aim of using the response surface method in this work. The novelty of this paper is using heavy feedstock different from other studies, utilizing simple reaction setup, comparison of two different aluminosilicate catalysts, comparison of impregnation of two different metals, and using response surface method to optimize the product distribution and find the best operating condition.

Experimental Method

Materials

The virgin Pyrolysis Fuel Oil (PFO) feedstock, which was introduced into the thermal cracking stage, is obtained from Maron Petrochemical Company. The cracked PFO is then used in the catalytic cracking stage as an upgraded feedstock. Properties of the cracked PFO have been presented in Table 1.

Table 1. The cracked PFO properties

Characteristic	Value
Color	Dark green
Density at 25 °C (g/cm^3)	1.0258
Viscosity at 37.8 °C (mm^2/s)	5.1255
Viscosity at 98.9 °C (mm^2/s)	1.3735
Refractive index at 37.8 °C	1.608
n-Heptane insoluble (wt. %)	1.1811

The nanoporous catalysts used in this study are Na-ZSM-5 and Al-MCM-41 (Tianjin Chemist Scientific). The typical properties of the catalyst samples have been introduced in Table 2.

Table 2. Properties of the origin catalyst samples

Characteristic	Na-ZSM-5	Al-MCM-41
Color	White powder	White powder
BET surface area (m^2/g)	320	820.5
Si/Al atomic ratio	38	59
Pore volume (cm^3/g)	-	0.94
Pore size (nm)	-	3.00
Al_2O_3 (wt. %)	-	3.3
Na_2O (wt. %)	0.04	-
Crystallinity (%)	97.5	-
Capacity of adsorption (n-Hexane, %)	0.94	-

Ammonium nitrate (Merck, Germany) has been employed in the ion-exchange step. $Fe(NO_3).9H_2O$ (Merck, Germany) and tetraethyl orthotitanate (Merck, Germany) are used as sources of iron and titanium, respectively. Deionized water and 2-propanol were used as solvents of iron and titanium sources, respectively, for the impregnation of catalyst.

Catalyst Preparation

At first, in order to prepare the acid form of zeolites, 4g of origin catalyst was dissolved in 100 ml of an aqueous solution of 1 molar ammonium nitrate. Then the slurry solution was stirred for 3 hours at 80 °C. The slurry solution of samples was filtered and then was dried in the oven for 12 hours at 110 °C, and then was calcined for 4 hours at 550 °C to prepare an acid form of catalyst. The acid form of Na-ZSM-5 and Al-MCM-41 were designated as H-ZSM-5 and H-MCM-41, respectively.

In order to impregnate the origin and acid forms of catalyst samples with Fe, the calculated amount of $Fe(NO_3).9H_2O$ was dissolved in 100 ml of deionized water and then 4g zeolite was added to the solution. The slurry solution was stirred for 1 hour at a temperature of 30-40 °C.

In order to impregnate the origin and acid forms of catalyst samples with Ti, the calculated amount of tetraethyl ortho titanate was dissolved in 100 ml of 2-propanol and then 4g of zeolite was added to the solution. The slurry solution was stirred for 30 min at room temperature.

The solvent of the obtained slurry solution was removed with a rotary evaporator under vacuum condition. The impregnated catalyst samples were dried in the oven for 12 hours at 110 °C and then were calcined for 4 hours at 550 °C.

Characterization of Catalyst

Small-angle XRD patterns were recorded on an X'Pert MPD diffractometer with CoKa radiation with wavenumber 1.78897 at 40 kV and 40 mA, and a scanning rate of 0.02 °/s. The origin sample of Al-MCM-41 zeolite was used as the reference for crystallinity comparison. The degree of crystallinity of modified samples was defined based on the main X-ray diffraction peak (2θ= 1.4–5.4) obtained from:

$$\text{Crystallinity} = \left[\frac{(\text{peak area of modified sample})}{(\text{peak area of reference sample})}\right] * 100\% \quad (1)$$

FT-IR spectra were recorded on a PerkinElmer Fourier transform infrared spectrometer at a resolution of 1 cm^{-1}. About 20 mg of each calcined samples were pressed into a self-supporting pellet without KBr dilution. Each wafer was placed into an infrared cell with KBr windows then measured at room temperature between4000and 400 cm^{-1}.

Compositions of the origin (Na-ZSM-5) and modified zeolite (Ti/H-MCM-41) were determined by X-ray fluorescence (XRF) spectrometer.

Catalytic Cracking Experiments

A schematic system of catalytic cracking of cracked PFO has been shown in Fig. 1. The flow of nitrogen was controlled with an F-1 flow meter. Nitrogen gas was preheated to reach 150 °C before the reaction. 50 g of the cracked PFO with a desirable amount of catalyst (2-5 g) was added to the reactor R-1. The reactions were carried out in a Pyrex round bottom glass flask with a capacity of 500 ml with a total residence time of 120 min under atmospheric pressure. An electric mantle was used to heat the reactor contents. The reactor was insulated with glass wool to minimize heat losses. The temperature of the reaction (360-400 °C) was controlled with an R-1 controller. The product gases obtained from catalytic cracking cooled in the condenser C-1 and two-stage ice-water bath. The liquid product was collected in the G-1 bottle and the gas product burned in a flare or analyzed by GC every 20 min.

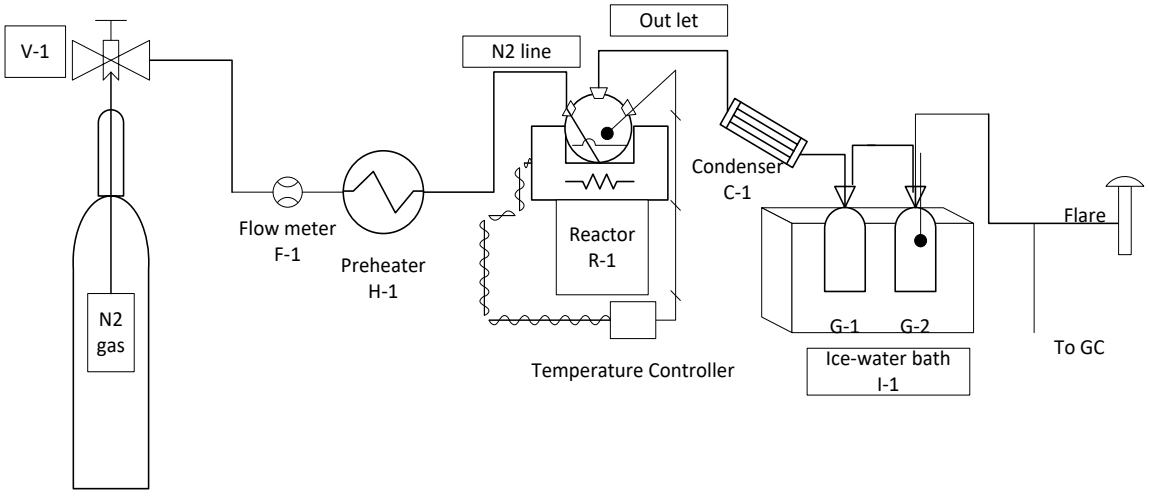

Fig. 1. Schematic system of catalytic cracking

Experimental Design

In order to reduce the number of experiments, preliminary tests were carried out firstly, to choose the best catalyst with the best catalytic activity to obtain the desired product distribution. Preliminary tests of catalytic cracking were carried out at a moderate temperature of 380 °C, a catalyst to feed ratio of 0.07, and a metal loading of 3%. The list of catalysts used in the preliminary tests has been shown in Table 3.

Table 3. List of catalysts used in preliminary tests

Catalyst	Ion exchange	Loading of Fe (wt. %)	Loading of Ti (wt. %)
Al-MCM-41	No	-	-
H-MCM-41	Yes	-	-
Fe/Al-MCM-41	No	3%	-
Fe/H-MCM-41	Yes	3%	-
Ti/Al-MCM-41	No	-	3%
Ti/H-MCM-41	Yes	-	3%
Fe,Ti/H-MCM-41	Yes	1.5%	1.5%
Na-ZSM-5	No	-	-
H-ZSM-5	Yes	-	-
Fe/H-ZSM-5	Yes	3%	-
Ti/H-ZSM-5	Yes	-	3%

After preliminary tests, the results were compared to choose the best catalyst. A five-level CCD was performed using statistical software (Design-Expert 7) to analyze the significance of experimental results and evaluate the importance order of independent factors and the interaction between independent variables. In this method, 3 key parameters of temperature of reaction, catalyst to feed ratio, and metal loading rate were used to obtain a polynomial model. The research goal was to optimize gas and liquid product distribution. To achieve this objective, increasing liquid product yield and decreasing viscosity of liquid product are selected as a measure of liquid quantity and quality, respectively. As a byproduct, the suitable gas product distribution was measured to increase total olefin yield. Other parameters have less importance than liquid product yield, the viscosity of the liquid product, and total olefin yield. Our experimental design includes 14 runs and a center point with 3 repetitions to evaluate the error in each experiment. Design parameters and levels are presented in Table 4.

Table 4. The design parameters, coded levels, and actual values used for experimental design

Parameter	Symbol	Actual values of coded levels				
		-α=-1.682	-1	0	+1	+α=+1.682
Temperature of reaction (°C)	A	360	368	380	392	400
Catalyst to feed ratio	B	0.04	0.522	0.07	0.878	0.1
Loading of metal (wt. %)	C	0	1	2.5	4	5

Results and Discussion Catalyst Characterization

XRD Patterns of Samples

Fig. 2 indicates XRD patterns of the H-ZSM-5 zeolite sample at 5° to 80°C. H-ZSM-5 catalyst exhibits all the typical peaks of ZSM-5 zeolite. Two peaks at 9.25° and 10.33° and 3 peaks at 26.91°, 27.15, and 27.65 verify the aluminosilicate structure of ZSM-5 zeolite. Washing, drying, and calcination of the catalyst sample at high temperature remove any impurities and NO_3^- ions from the catalyst after ion exchange. The results of XRD patterns of H-ZSM-5 zeolite compared to Na-ZSM-5 origin zeolite of previous investigations [25].

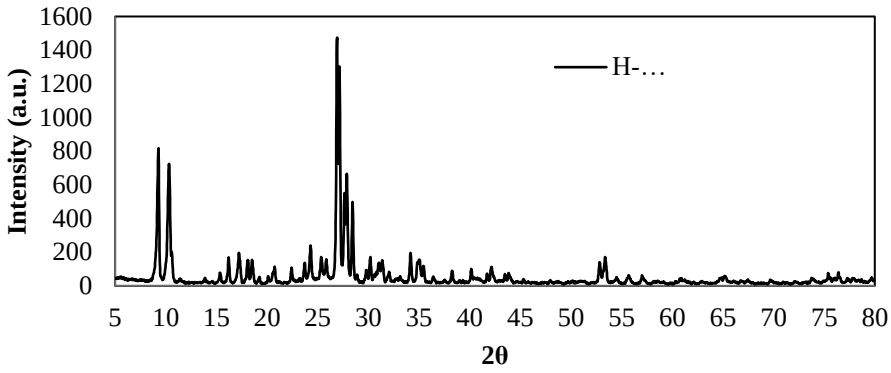

Fig. 2. XRD pattern of H-ZSM-5 sample

Fig. 3 shows the small-angle XRD patterns of origin and modified MCM-41 zeolites samples between 1.5° to 12°. All the MCM-41 catalysts exhibit typical peaks of MCM-41 zeolite, indicating that the aluminosilicate structure of MCM-41 zeolite is remained intact after ion exchange, impregnation, or both. However, the intensity of peaks may change depending on the employed modification method. Relative obtained crystallinity of Al-MCM-41 (reference sample), H-MCM-41, Fe/Al-MCM-41, and Ti/H-MCM-41 were 100%, 96.4%, 85.7%, and 81.4%, respectively. The ion exchange method has little effect on decreasing the relative crystallinity, However, the impregnation for 3% of metal loading to the surface of zeolites decreases the relative crystallinity to 85.7%. When both modification methods were used, the relative crystallinity decreases even more, so that the relative crystallinity of Ti/H-MCM-41 is 81.4%.

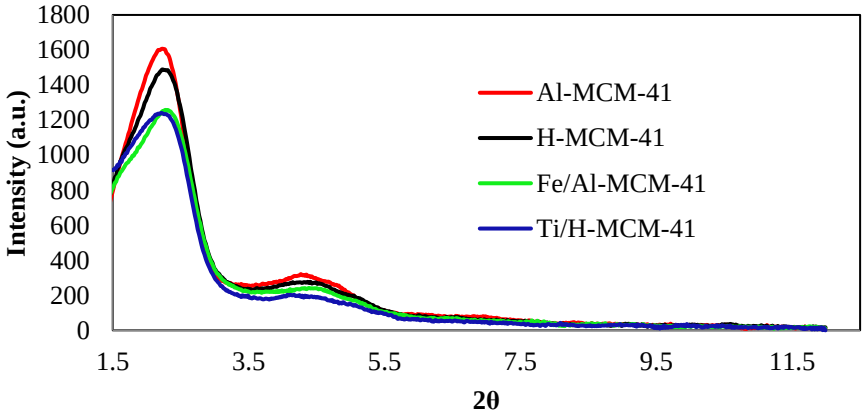

Fig. 3. Small-angle XRD patterns of MCM-41 zeolite samples

FT-IR Spectrum of Samples

Fig. 4 shows the FT-IR spectrum of H-ZSM-5 zeolite at room temperature between 4000 cm^{-1} to 400 cm^{-1}. The bands around 3650 cm^{-1}, 3443.28 cm^{-1}, and 1630.66 $cm^{-1}$are attributed to -OH stretching of acid sites of the ZSM-5 zeolite. The bands at 1087.16 cm^{-1}, 796.07 cm^{-1}, 622.68 cm^{-1}, and 458.97 cm^{-1} are assigned to stretching vibration of the T-O-T (T=Si/Al) group. The band at 1226 $cm^{-1}$is attributed to the outside banding of the aluminosilicate structure of ZSM-5 and the band at 546.57 $cm^{-1}$is attributed to pentasil 5-ring which indicates the structure of ZSM-5. This FT-IR spectrum proves the structure of ZSM-5.

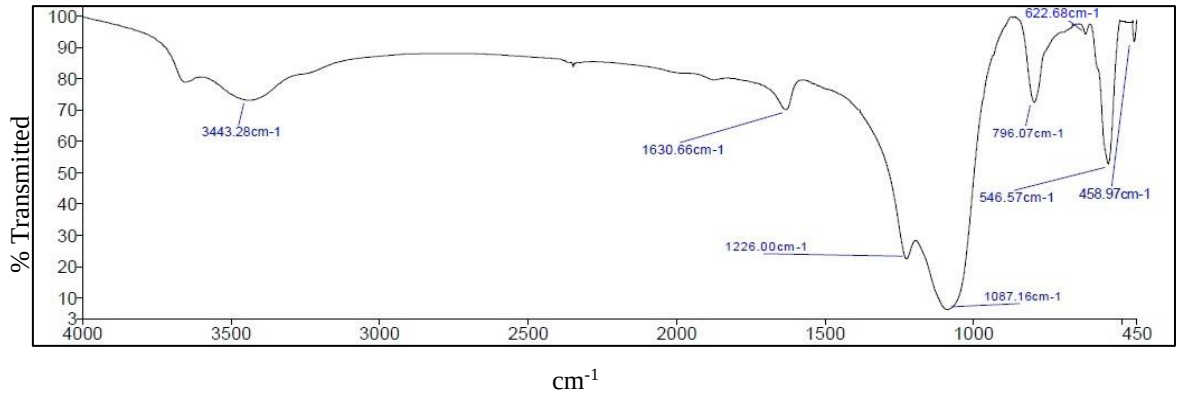

Fig. 4. The FT-IR spectrum of H-ZSM-5 zeolite between 4000-400 cm^{-1}

Fig. 5 shows the FT-IR spectrum of MCM-41 zeolite samples at room temperature between 4000-400 cm^{-1}. The bands at 3434 cm^{-1} and 3746 $cm^{-1}$are related to the stretching vibration of the -OH and Si-OH groups are indicative of the acidity of catalyst samples. Ion exchange and impregnation of titanium both increased the acidity of zeolite samples. The order of acidity of catalyst is Ti/H-MCM-41>H-MCM-41>Al-MCM-41, which agrees with the FT-IR spectrum of samples. The bands at 1078 cm^{-1}, 807 cm^{-1}, and 458 cm^{-1} are attributed to the stretching vibration of the T-O-T (T=Si/Al) group. This FT-IR spectrum of the catalyst samples proves the aluminosilicate structure of MCM-41 catalysts.

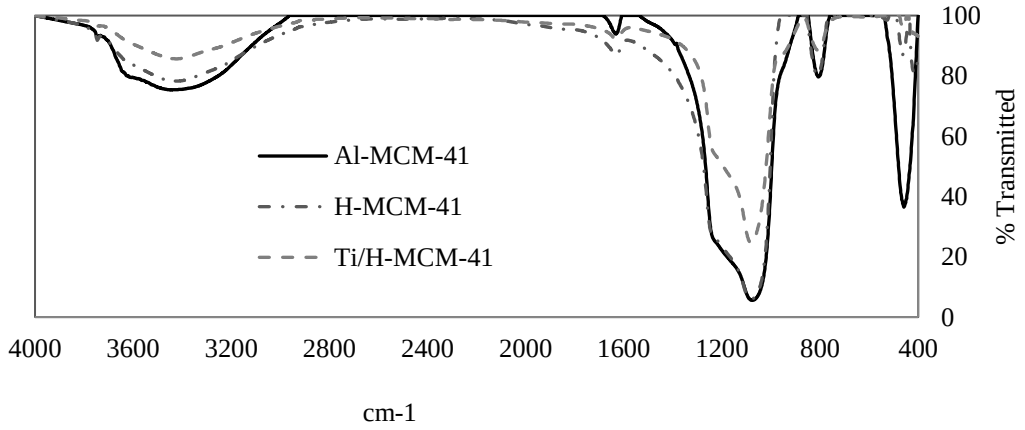

Fig. 5. The FT-IR spectrum of MCM-41 zeolite samples between 4000-400 cm^{-1}

XRF Analysis of Samples

Table 5 shows the composition of catalyst samples determined by XRF analysis. Most of the zeolites include silicon oxide and aluminum oxide with a small amount of iron(III) oxides. The calculated amount of titanium was loaded into the surface of Ti/H-MCM-41catalyst, accurately. Traces of Na, P, Cl, K, Ti, Ni, Cu, and Zr are evident in the structure of Na-ZSM-5 zeolite and traces of Na, S, K, Ni, Sr, Zr, and Ag are observed in the structure of Ti/H-MCM-41 catalyst. For comparison of the main composition of ZSM-5 and MCM-41 based catalysts XRF analysis of Na-ZSM-5 and Ti/H-MCM-41 were done. Also, the XRF analysis of the Ti/H-MCM-41 catalyst was done to be sure that the amount of impregnated Ti loading on the catalyst surface was done accurately.

Table 5. The composition of catalyst samples determined by XRF analysis

Composition (wt. %)	**SiO_2**	**Al_2O_3**	**Fe_2O_3**	**TiO_2**	**MgO**	**SO_3**	**Cr**	**P_2O_5**
Na-ZSM-5	95.357	4.306	0.155	-	0.100	0.082	-	-
Ti/H-MCM-41	89.455	5.226	0.521	4.469	0.117	-	0.147	0.065

Preliminary Tests of Catalytic Cracking of Cracked PFO

Fig. 6a-b show the liquid, solid, and gas product yields using ZSM-5 base and MCM-41 base catalysts, respectively, obtained from low-temperature catalytic cracking of cracked PFO at 380 °C. In the absence of a catalyst (blank), the liquid and gas productyieldswere85.03% and 5.38%, respectively. However, when the catalyst was used, the liquid product yield reduced while the gas product yield increased in all cases which means catalyst increases the cracking of cracked PFO. In the presence of a catalyst, liquid and gas yields were between 71.65% to 81.62% and 7.42% to 20.02%, respectively. The order of liquid and gas yield, in the presence of ZSM-5 base catalysts, was: Blank>H-ZSM-5>Na-ZSM-5>Fe/H-ZSM-5>Ti/H-ZSM-5 and Ti/H-ZSM-5>Fe/H-ZSM-5>H-ZSM-5>Na-ZSM-5> Blank, respectively. It shows the significant effect of ion exchange and impregnation with iron and titanium on increasing of light product distribution. The order of liquid and gas yield, in the presence of MCM-41base catalysts, was: Blank>Ti/H-MCM-41>H-MCM-41>Fe/Al-MCM-41>Al-MCM-41>Fe/H-MCM-41>Fe,Ti/H-MCM-41>Ti/Al-MCM-41and Ti/Al-MCM-41>Fe,Ti/H-MCM-41>Al-MCM-41>Fe/H-MCM-41>Fe/Al-MCM-41>H-MCM-41>Ti/H-MCM-41> Blank, respectively. Among the MCM-41 base catalysts, when the liquid yield and quality was high, the gas yield was low and when the liquid yield and quality was low, the gas yield was high. Both indicate the important role of catalytic cracking in the production of light products. Among the employed catalysts, Ti/H-MCM-41 had the highest liquid yield and Ti/Al-MCM-41 had the highest gas yield, which shows the significant effect of impregnating with titanium on catalytic cracking of cracked PFO.

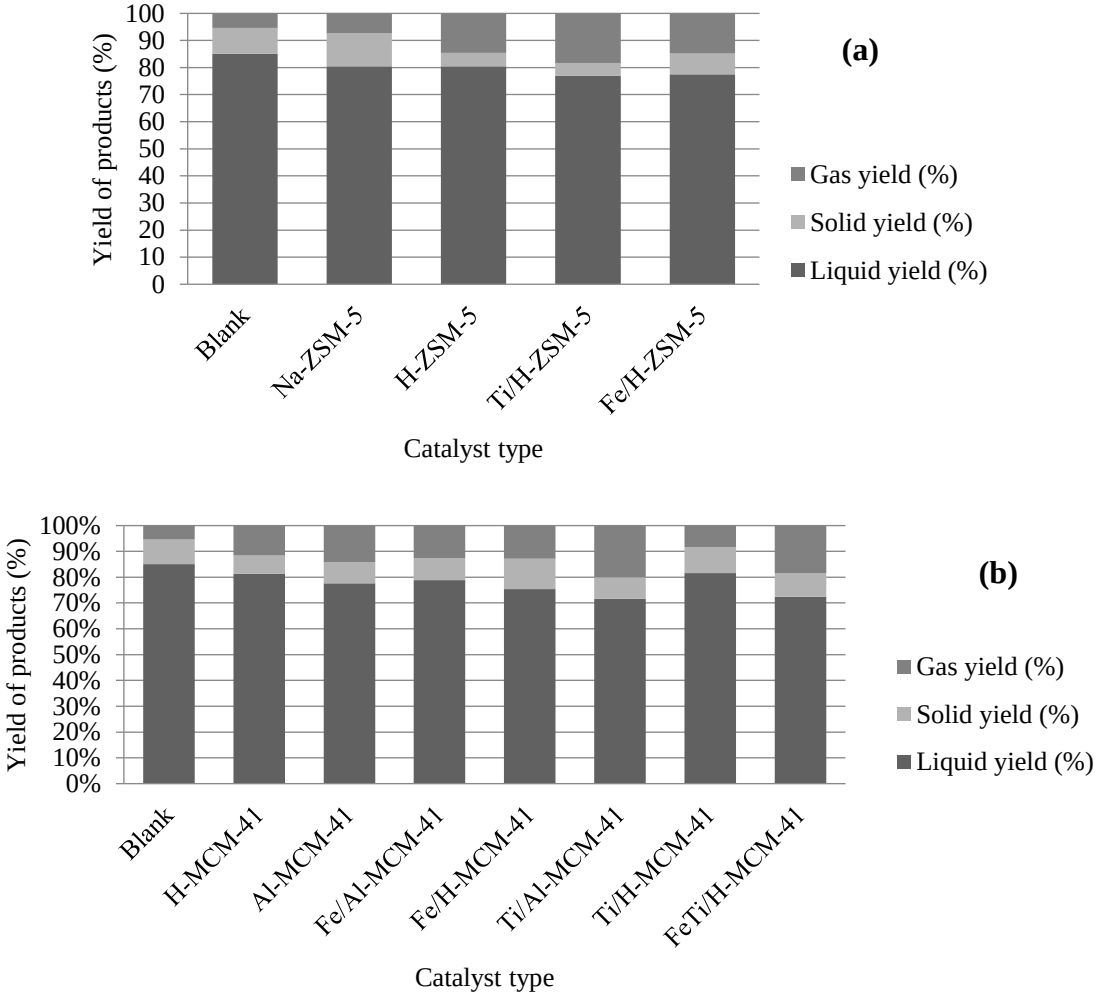

Fig. 6. The liquid, solid and gas yield of products(a) using ZSM-5 base catalysts (b) using MCM-41 base catalysts

Liquid Product Analysis

Table 6 presents viscosity, density, and refractive index of the liquid product obtained from low-temperature catalytic cracking of cracked PFO at 380 °C. All the liquid products had viscosity, density, and refractive indices lower than the feed which shows the effect of catalytic cracking on improving liquid quality. Among the catalysts used in the preliminary tests of catalytic cracking of cracked PFO, viscosity, density, and refractive indices of the liquid product, in the presence of Na-ZSM-5, H-ZSM-5, Fe/H-MCM-41, and Ti/Al-MCM-41 catalyst samples were more than those of the liquid product of Blank. It shows that the undesirable quality of liquid products obtained from these catalyst samples and the catalytic cracking did not have enough effect on increasing the quality of the liquid product. However, the viscosity, density, and refractive indices of liquid product using the H-MCM-41, Al-MCM-41, Ti/H-ZSM-5, Fe/H-ZSM-5, Fe/Al-MCM-41, Ti/H-MCM-41, and Fe, Ti/H-MCM-41 catalyst samples were less than those of the liquid product of Blank. It shows the significant effect of the catalytic cracking on improving the quality of the liquid product. The order of the viscosity, density, and refractive indices were Fe/H-MCM-41>Ti/Al-MCM-41>H-ZSM-5>Na-ZSM-5>Blank>Fe/H-ZSM-5>Ti/H-ZSM-5>Al-MCM-41>H-MCM-41>Fe,Ti/H-MCM-41>Fe/Al-MCM-41>Ti/H-MCM-41. Among the used catalysts, Ti/H-MCM-41 had the lowest value of viscosity, density, and refractive index. It shows that it had the highest catalytic activity in the production of light liquid products from heavy feedstocks, such as PFO.

Table 6. Viscosity, density, and refractive indices of the liquid product of preliminary tests of catalytic cracking of cracked PFO

Catalyst	Viscosity at 37.8 °C (mm^2/s)	Density at 25 °C (g/cm^3)	Refractive index at 37.8 °C
Blank	3.6135	1.0125	1.600
Na-ZSM-5	3.6280	1.0144	1.600
H-ZSM-5	3.6506	1.0164	1.602
H-MCM-41	3.4739	1.0077	1.594
Al-MCM-41	3.5763	1.0096	1.595
Ti/H-ZSM-5	3.5737	1.0096	1.599
Fe/H-ZSM-5	3.5976	1.0115	1.6
Fe/Al-MCM-41	3.2744	0.9875	1.574
Fe/H-MCM-41	4.8659	1.0202	1.607
Ti/Al-MCM-41	3.9456	1.0183	1.603
Ti/H-MCM-41	3.1901	0.9788	1.574
Fe,Ti/H-MCM-41	3.4215	1	1.592

Gas Chromatography of Gas Products

Fig. 7a-b show the total light olefin of gas product distribution and temperature during the reaction, for origin and acid form of ZSM-5 and MCM-41 and impregnated form of ZSM-5 and MCM-41, respectively. Total light olefin is mostly composed of propylene and ethylene. After 45 min, when the temperature reached its final point, all the catalysts, except ZSM-5 base catalysts, had the highest catalytic activity for the production of the light olefin. After 45 min, MCM-41 base catalysts, in comparison with ZSM-5 base catalysts, had a high catalytic activity for the production of the light olefin. Thereafter, the yield of total light olefin in MCM-41 base catalysts decreased and the yield of total light olefin in ZSM5 base catalysts mostly increased. The flow of gas products in 5, 25, and 45 minutes after initiation of the process were much higher than that of 65, 85, and 105. It shows that high catalytic activity in 45 minutes after the start of the experiment is more important than other times of reaction. The yield of the light olefin after 45 min drops suddenly by using Al-MCM-41 and H-MCM-41 as catalysts,

However, the impregnated MCM-41 based catalysts decrease the yield of the light olefin and show the effect of impregnating of MCM-41 base catalysts with iron and titanium on increasing the stability of the catalyst and decreasing of coke formation during the reaction. After 45 min, among all the employed catalysts, H-MCM-41, Al-MCM-41, Ti/H-MCM-41, and Ti/Al-MCM-41 had the highest total olefin yield, respectively.

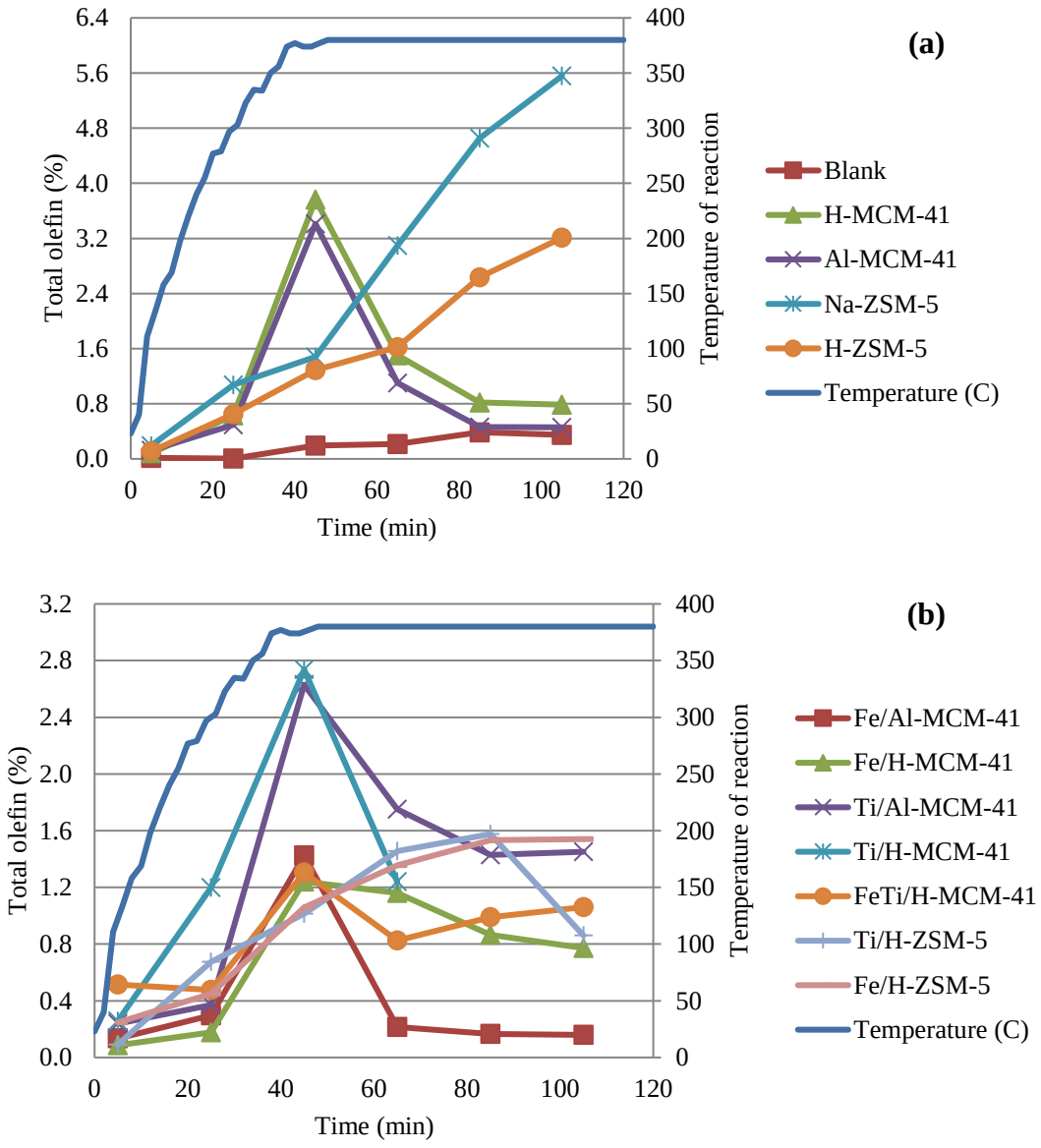

Fig. 7. Temperature of the reaction during the reaction progress and the total light olefin of produced gas (a) using origin and acid form of ZSM-5 and MCM-41 base catalysts and (b) using the impregnated form of ZSM-5 and MCM-41 base catalysts

High yield of light olefin as a result of using the ZSM-5 base catalysts emphasizes that ZSM-5 base catalysts are very suitable for the production of a light olefin such as ethylene and propylene however most of the product remains in the liquid state and the liquid product obtained from ZSM-5 base catalysts do not have the desirable quality to be used as fuels, such as gasoline and light gasoil. Ion exchange creates intracrystalline mesopores in the aluminosilicate catalyst which could help metal species to transfer easily into aluminosilicate catalyst crystals and shorten the distance between acid sites and metal active sites. Also, intracrystalline mesopores could improve the diffusion and adsorption properties of the reactant

molecules. Impregnation of metal species reduces the total amount of acid sites which could increase the yield of total olefin in the gas product. In comparison to Ti and Fe impregnation, two metal species have the same performance in the catalytic reaction. But Ti has better resistance in the reaction condition in high temperature which means that the bond of TiO_2 molecules with the aluminosilicate catalyst is stronger than the Fe_2O_3 molecules.

Fig. 8a-b show the total paraffin of gas product distribution and temperature, during the reaction process, for origin and acid form of ZSM-5 and MCM-41 and impregnated form of ZSM-5 and MCM-41, respectively. Total paraffin is mainly composed of methane, ethane, propane, and isomers of butane. The share of lighter products, such as methane and ethane, is more than the share of propane and isomers of butane. After 45 min, when the temperature reached its final point, all the MCM-41 base catalysts had a high catalytic activity for the production of kinds of paraffin, but ZSM-5 base catalysts had a low catalytic activity for the production of different forms of paraffins. It emphasize that, for production of light paraffinic products, ZSM-5 base catalysts are not suitable and ZSM-5 base catalysts are selective ones which only produce light olefins, such as ethylene and propylene, because of micropore structure and small cages of ZSM-5 catalyst; however, MCM-41 base catalysts have mesoporous structures with large cages for easy access and diffusion of large molecules of hydrocarbons. In the presence of Al-MCM-41 and H-MCM-41 catalysts, the yield of total paraffin suddenly dropped after 45 min, However, the application of impregnated MCM-41 based catalysts, as total light olefin, slightly decreased total yield of the paraffin. In comparison to the ZSM-5 and MCM-41 based catalysts, MCM-41 based catalysts have a mesoporous structure that suitable for molecules of heavy feedstocks. Ion exchange decreases the acidity of the catalysts and improves the performance of reaction. According to the results, Ti increases active metal sites that improve the cracking of large molecules. So the Ti/H-MCM-41 catalyst chosen for the secondary tests.

Experimental Design Tests of Catalytic Cracking of Cracked PFO

After preliminary tests, 3%Ti/H-MCM-41 was selected as the best catalyst for upgrading the cracked PFO. Numerical values of the three important parameters such as liquid, solid, gas product yields, and properties of liquid products for each run are listed in Table 7.

In each run of cracked PFO catalytic cracking, the distribution of gas products includes dry gas, LPG, and C5+ include methane, ethane, propane, isomers of butane, and a larger amount of aromatic compounds, respectively, which is listed in Table 8. Most of the feed include aromatics such as benzene, toluene, and isomers of xylenes. Aromatic compounds are cracked so hard by catalytic cracking and easily evaporated because of low boiling point and volatility properties, therefore most of the gas products include aromatic compounds.

Data Analysis

Data obtained from experimental design tests of catalytic cracking of cracked PFO were statistically analyzed to identify the important parameters for each response. Analysis of variance (ANOVA) of the experimental design tests was carried out to choose the best model. After checking out all models, it was found that a reduced 2FI model for liquid yield and

viscosity of the liquid product as well as a reduced quadratic model for the total olefin yield of gas product could have the best fit to the experimental design test data. Three main parameters are A, B, and C which indicate the temperature of reaction (°C), the catalyst to feed ratio, and the loading of metal (%), respectively. The liquid yields' response involved the parameters of A, B, C, and BC and viscosity of liquid products' response involved the parameters of A, B, C, AB, and BC and the total olefin yield of gas products' response involved the parameters of A, B, C, A^2, B^2, and C^2. The summary of the ANOVA test results for the three important responses is presented in Table 9.

Table 7. Numerical values of each experimental design tests' parameter, the yield of products and properties of the liquid product of catalytic cracking of cracked PFO

Run	Temperature (°C)	Catalyst to feed ratio	Ti loading (wt.%)	Liquid yield (wt.%)	Solid yield (wt.%)	Gas yield (wt.%)	Viscosity at 37.8 °C (mm^2/s)	Density at 25 °C	Refractive index at 37.8 °C
1	392	0.0522	4.0	84.66	12.88	2.46	3.1744	0.9774	1.574
2	380	0.0400	2.5	76.91	6.44	16.65	3.3983	0.9888	1.5845
3	400	0.0700	2.5	87.62	4.93	7.45	3.3897	0.9872	1.581
4	380	0.0700	5.0	80.28	11.68	8.04	3.1470	0.9761	1.574
5	392	0.0878	4.0	75.55	10.84	13.61	3.4120	0.9894	1.5845
6	380	0.0700	2.5	77.87	11.94	10.28	3.2249	0.9799	1.5765
7	368	0.0522	1.0	75	16.66	8.35	3.3743	0.9856	1.5815
8	368	0.0878	4.0	69.8	5.62	24.58	3.0869	0.9722	1.569
9	380	0.0700	2.5	81.4	11.73	6.87	3.2765	0.9812	1.577
10	392	0.0522	1.0	80.72	12.5	6.79	3.2848	0.9820	1.579
11	392	0.0878	1.0	81.22	8.39	10.39	3.2751	0.9818	1.578
12	360	0.0700	2.5	72.7	9.21	18.09	3.3047	0.9869	1.5825
13	368	0.0522	4.0	76.43	11.11	12.45	3.1710	0.9769	1.575
14	380	0.0700	0.0	81.34	7.14	11.25	3.4739	1.0077	1.594
15	380	0.0700	2.5	78.27	11.24	10.49	3.3818	0.9870	1.582
16	368	0.0878	1.0	73.04	16.59	10.37	3.1702	0.9768	1.574
17	380	0.1000	2.5	83.56	12.79	3.65	3.1686	0.9751	1.573

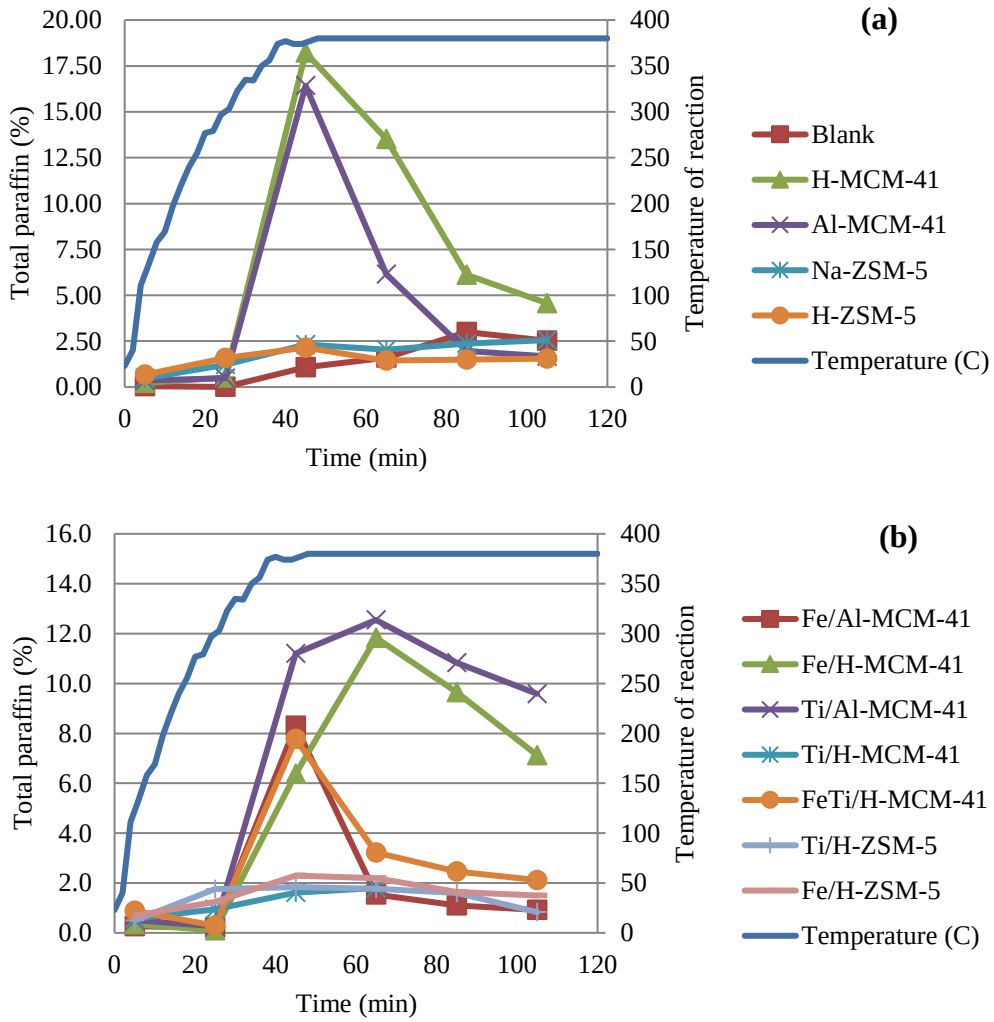

Fig. 8. Temperature during reaction process and total paraffin of gas produced (a)using origin and acid form of ZSM-5 and MCM-41 base catalysts (b)using the impregnated form of ZSM-5 and MCM-41 base catalysts

Table 8. Distribution of gas product for experimental design tests of catalytic cracking of cracked PFO

Run	Ethylene	Propylene	C2= +C3=	Total Olefins	Dry Gas	LPG	Total Paraffins	C5+	Total
1	0.60	0.90	1.51	2.02	5.57	0.78	6.35	91.63	100
2	0.46	0.72	1.18	1.58	4.47	0.83	5.57	92.86	100
3	0.67	1.01	1.68	2.27	8.30	0.87	9.17	88.56	100
4	0.87	1.30	2.18	2.91	9.11	0.90	1.01	87.08	100
5	0.80	1.20	2.01	2.45	9.60	0.94	10.54	87.01	100
6	1.51	1.93	3.43	3.58	17.01	1.92	18.93	77.50	100
7	0.59	0.87	1.46	1.96	6.67	1.13	7.89	90.15	100
8	0.98	1.54	2.53	3.38	11.11	1.59	12.70	83.92	100
9	0.94	1.38	2.32	3.06	11.67	1.28	12.95	83.99	100
10	0.33	0.69	1.02	1.13	2.89	1.03	3.92	94.95	100
11	1.17	1.77	2.94	4.12	12.11	1.47	13.58	82.31	100
12	0.61	0.97	1.58	2.10	7.17	1.13	8.31	89.59	100
13	0.59	0.94	1.53	1.92	6.14	0.90	7.05	91.04	100
14	1.30	2.02	3.32	3.77	15.54	2.69	18.23	78.01	100
15	1.21	1.81	3.03	3.99	13.57	1.52	15.09	80.92	100
16	0.93	1.61	2.54	3.41	10.22	1.52	11.74	84.85	100
17	1.54	2.36	3.90	5.57	17.15	1.78	18.93	75.49	100

Table 9. Summary of analysis of variance (ANOVA) for important responses

Response		Sum of squares	DOF	Mean square	F-value	p-value	Lack of fit
Liquid yield	Model	235.68	4	58.92	6.41	0.0053	0.3041
	Residuals	110.30	12	9.19			
Viscosity of liquid product	Model	0.13	5	0.026	3.76	0.0314	0.5627
	Residuals	0.076	11	0.006929			
Total olefin yield of gas product	Model	16.78	6	2.80	7.98	0.0024	0.4096
	Residuals	3.51	10	0.35			

Table 10 displays the ANOVA results at 95% confidence levels for liquid yield response. According to the p-value, as a tool for evaluation of the significance level of parameters, the impact of the temperature of reaction (A) is significant with p-value < 0.05. In addition, the model variable is insignificant with the p-value larger than 0.05, so catalyst to feed ratio (B), loading of metal (C), and interaction between catalyst to feed ratio and loading of metal (BC) are insignificant for liquid yield response. Based on the values of the monomial coefficients derived from the model, p(A) = 0.0005, p(B) = 0.6011 and p(C) = 0.6433, the decreasing order of the influence of independent variables on liquid yield response is the temperature of reaction > catalyst to feed ratio > loading of metal.

Table 10. Coefficients of regressions and their significances for liquid yield response

Factor	Coefficient estimate	Degree of freedom	Standard error	F-value	95% confidence interval Low	95% confidence interval High	p-value
Intercept	78.60	1	0.74	-	77.00	80.21	-
A	3.88	1	0.82	22.35	2.09	5.67	0.0005
B	-0.44	1	0.82	0.29	-2.23	1.35	0.6011
C	-0.39	1	0.82	0.23	-2.18	1.40	0.6433
BC	-1.79	1	1.07	2.77	-4.12	0.55	0.1217

Table 11 displays the ANOVA results at 95% confidence levels for the viscosity of liquid product response. According to the p-value, as a tool for evaluation of the significance level of parameters, the impact of loading of metal (C) is significant with p-value < 0.05. In addition, the model variable is insignificant with the p-value larger than 0.05, so the temperature of reaction (A), catalyst to feed ratio (B), the interaction between the temperature of reaction and

catalyst to feed ratio (AB) and interaction between catalyst to feed ratio and loading of metal (BC) are insignificant for the viscosity of liquid product response. Based on the values of the monomial coefficients derived from the model, p(A) = 0.1418, p(B) = 0.1745 and p(C) = 0.0233, the decreasing order of the influence of independent variables on the viscosity of liquid product response is the loading of metal > temperature of reaction > catalyst to feed ratio. Table 12 displays the ANOVA results at 95% confidence levels for the total olefin yield of gas product response. According to the p-value, as a tool for evaluation of the significance level of parameters, the impact of catalyst to feed ratio (B) and the second order of temperature of reaction (A^2) are significant with p-value < 0.05. In addition, the model variable is insignificant with the p-value larger than 0.05, so the temperature of reaction (A), loading of metal (C), the second order of catalyst to feed ratio (B^2) and the second order of loading of metal (C^2) are insignificant for total olefin yield of gas product response. Based on the values of the monomial coefficients derived from the model, p(A) = 0.7679, p(B) = 0.0001 and p(C) = 0.3190, the decreasing order of the influence of independent variables on total olefin yield of gas product response is the catalyst to feed ratio> loading of metal> temperature of reaction.

Eq. 2-4 were obtained from the experimental design tests of catalytic cracking of cracked PFO using Design-Expert software.

$$\text{Liquid yield } (\%) = +78.60 + 3.88A - 0.44B - 0.39C - 1.79BC \quad (2) \tag{2}$$

$$\text{Viscosity of liquid product } (mm^2/s) = +3.28 + 0.036A - 0.033B - 0.059C + 0.065AB + 0.046BC \tag{3}$$

$$\text{Total olefin yield of gas product } (\%) = +3.57 - 0.049A + 0.95B - 0.17C - 0.58A^2 - 0.090B^2 - 0.17C^2 \tag{4}$$

Where A, B, and C are the temperature (°C), the catalyst to feed ratio, and loading of Ti (%).

Fig.9a-b shows contour plots of the predicted liquid yield constructed by Eq. 2 as the function of temperature (°C) and catalyst to feed ratio, loading of Ti (%), and temperature (°C), respectively. In Eq. 2, coefficient of A is larger than other coefficients of other parameters; i.e. liquid yield of product is mainly affected by the temperature of the reaction. Increasing the temperature increases the liquid yield of the product, however increasing catalyst to feed ratio or the loading of Ti decreases the liquid yield slightly; however, a catalyst to feed ratio and loading of Ti affect the viscosity reduction to obtain the lighter liquid product.

Table 11. Coefficients of regressions and their significances for viscosity of liquid product response

Factor	Coefficient estimate	Degree of freedom	Standard error	F-value	95% confidence interval Low	95% confidence interval High	p-value
Intercept	3.28	1	0.020	-	3.23	3.32	-
A	0.036	1	0.023	2.50	-0.014	0.085	0.1418
B	-0.033	1	0.023	2.11	-0.082	0.017	0.1745
C	-0.059	1	0.023	6.93	-0.11	-9.726E-003	0.0233
AB	0.065	1	0.029	4.81	-2.611E-004	0.13	0.0508
BC	0.046	1	0.029	2.43	-0.019	0.11	0.1470

Fig. 10a-b show contour plots of the predicted viscosity of liquid product constructed by Eq. 3, as the function of the loading of Ti (%), temperature(°C), a catalyst to feed ratio, and loading of Ti(%), respectively. Negative coefficients of B and C in Eq. 3 show that catalyst to feed ratio and the loading of Ti had a positive effect on the viscosity reduction. Increasing temperature increases the liquid yield and viscosity; however, the increasing catalyst to feed ratio and the loading of Ti decrease liquid yield and viscosity. Conditions of three important parameters are optimized to maximize the liquid yield with high quality of the liquid product, using an experimental design.

Table 12. Coefficients of regressions and their significances for total olefin yield of gas product response

Factor	Coefficient of estimate	Degree of freedom	Standard error	F-value	95% confidence interval Low	95% confidence interval High	p-value
Intercept	3.57	1	0.34	-	2.81	4.33	-
A	-0.049	1	0.16	0.092	-0.41	0.31	0.7679
B	0.95	1	0.16	35.74	0.60	1.31	0.00001
C	-0.17	1	0.16	1.10	-0.53	0.19	0.3190
A^2	0.58	1	0.18	10.84	-0.97	-0.19	0.0081
B^2	-0.090	1	0.18	0.26	-0.48	0.30	0.6230
C^2	-0.17	1	0.18	0.96	-0.57	0.22	0.3511

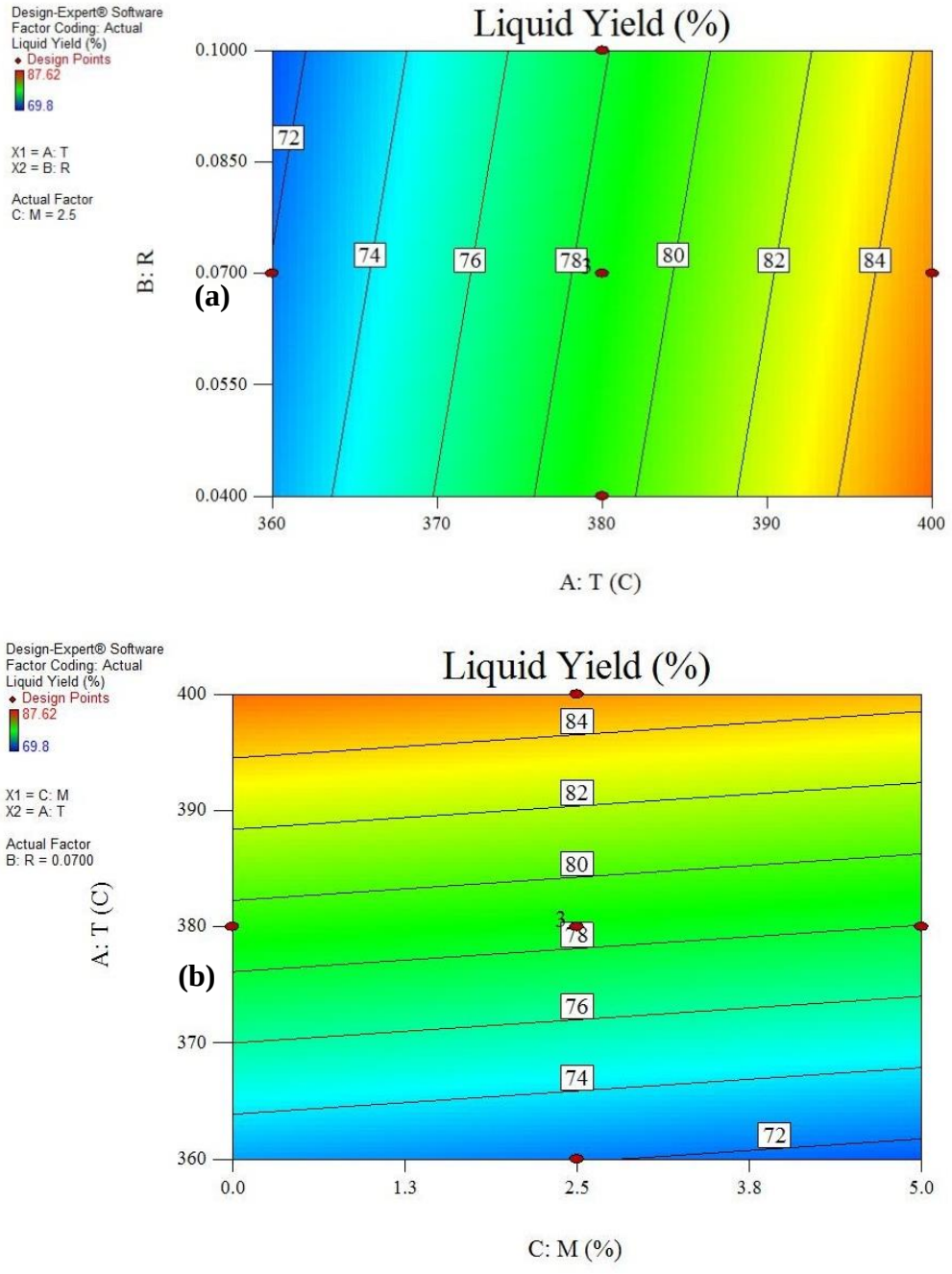

Fig. 9. Contour plots of the predicted liquid yield as the function of (a)temperature (°C) and catalyst to feed ratio (b) loading of Ti (%) and temperature (°C)

Fig. 11a-b show contour plots of the predicted total olefin of gas product constructed by Eq. 4 as the function of temperature(°C) and catalyst to feed ratio, loading of Ti (%) and temperature(°C), respectively. At the same time of high-quality liquid production, after 45 min, the gas product was analyzed with a gas chromatography instrument to optimize the distribution of liquid and gas products. At an average temperature, between 370-390 °C, the production of light olefins, such as ethylene and propylene, improved. An increasing catalyst to feed ratio increases the total olefin yield of the gas product, as well. In Fig. 11b, the area inside contour of 3.5 shows a suitable value of loading of Ti which is between 0.75-2.75 %.

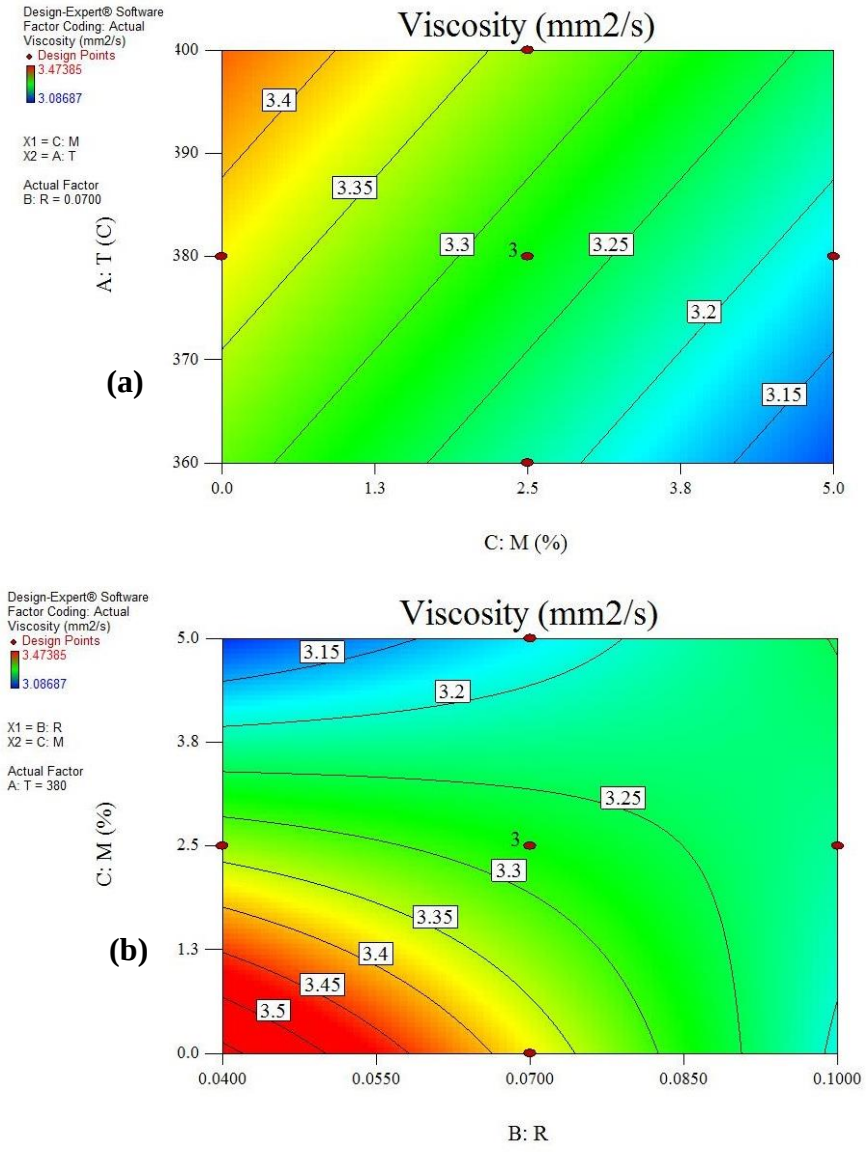

Fig. 10. Contour plots of the predicted viscosity as the function of (a)loading of Ti(%) and temperature(°C) and (b) catalyst to feed ratio and loading of Ti (%)

Fig. 12 shows the desirability factor for the maximum of liquid yield and total olefin of gas product and a minimum of viscosity. To obtain the optimum value of different parameters, the desirability factor in the Expert Design software utilized. The experimental design is to produce a high amount of liquid with low viscosity to maximize the gasoline yield. The maximum yield of total olefin of the gas product is the second aim as the byproduct. In Fig. 12, the area with values above 0.8 is the optimum condition for the experimental design test. Under optimum condition, the temperature, catalyst to feed ratio, and loading of Ti are between 370-390 °C, 0.085-0.1, and 1-3 %, respectively.

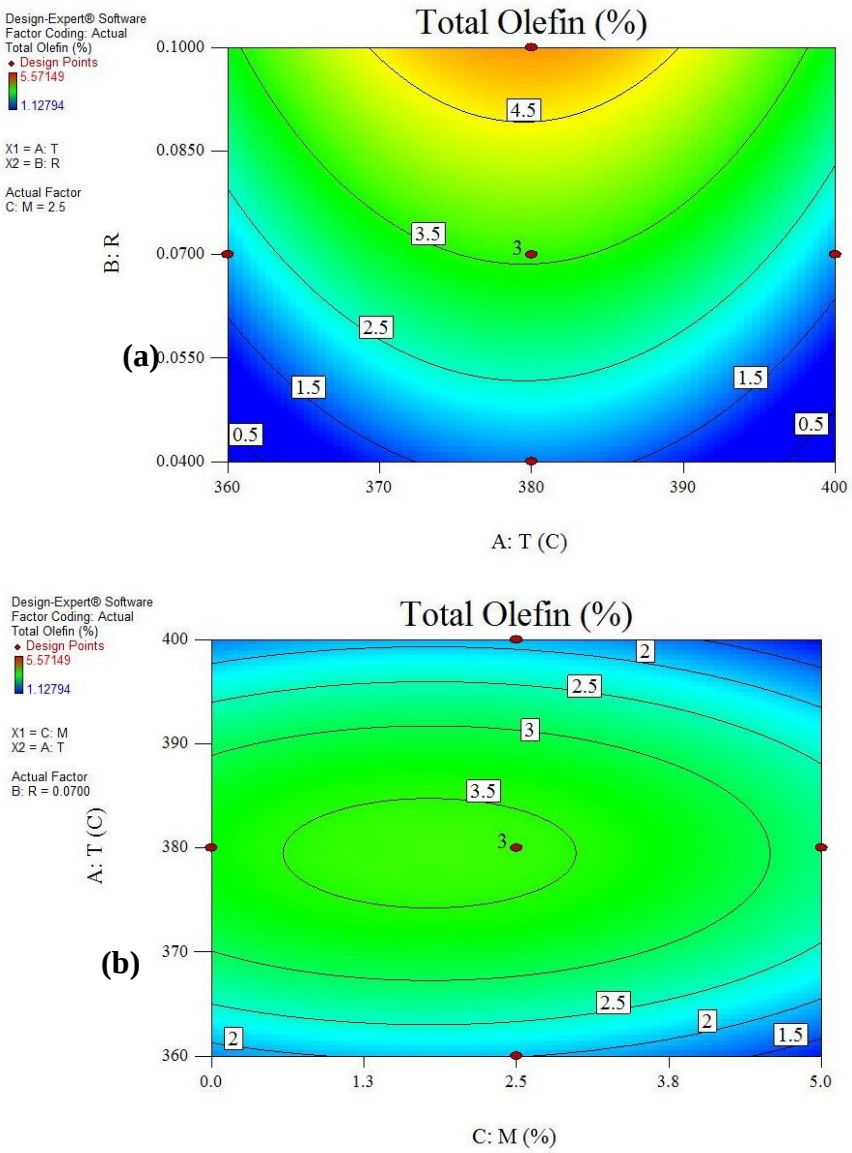

Fig. 11. Contour plots of predicted total olefin of gas product as the function of (a)temperature(°C) and catalyst to feed ratio and (b) loading of Ti (%) and temperature(°C)

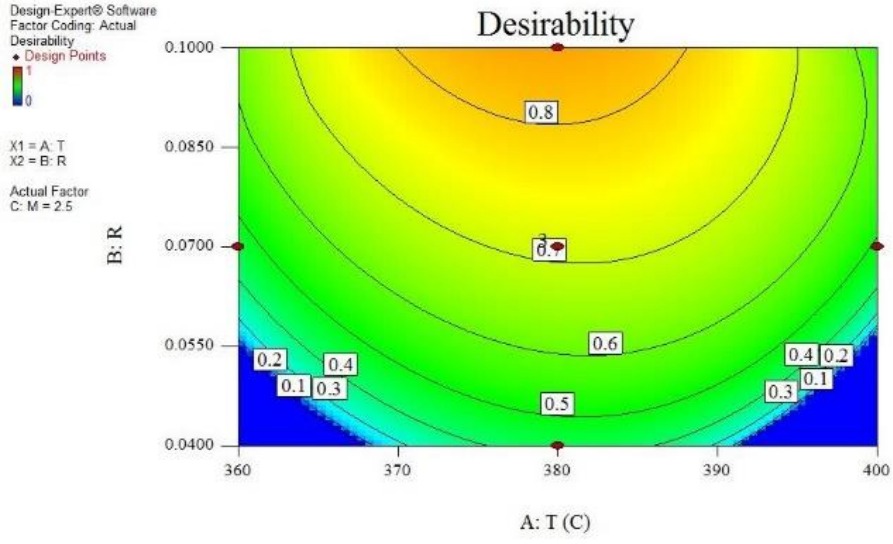

Fig. 12. The desirability factor for the maximum liquid yield and total olefin of gas product and minimum of the viscosity

Liquid Product Analysis

Table 13 exhibits liquid product high-performance liquid chromatography (HPLC) of the optimum condition of the experimental design tests (Run 17). Almost 85% of the liquid product is iso-paraffins and aromatics which are very useful hydrocarbons fuels, such as gasoline and gas oil with high octane and cetane number, respectively. Nearly 26 wt. % of the liquid product is in the range of gasoline (C_5-C_{10}) and the rest is in the range of light gas oil (C_{11}-C_{16}). The average molecular weight of the liquid product is 156.4 g/cm^3 which is near the molecular weight of $C_{11}H_{24}$.

Table 13. Liquid product analysis of the optimum condition of the experimental design tests

Type of hydrocarbons	Carbon Number	Weight (%)	Volume (%)	Mole (%)
Aromatics	6	5.591	5.052	11.194
	7	5.264	4.825	8.936
	8	2.976	2.725	4.384
	9	2.688	2.311	3.537
	10	3.862	3.515	4.500
	11	5.723	4.883	6.182
	12	5.434	5.000	5.238
	14	0.087	0.081	0.072
	15	0.087	0.081	0.066
	Sum	31.712	28.473	44.109
Iso-paraffins	6	0.343	0.417	0.623
	7	0.079	0.093	0.123
	10	0.685	0.744	0.753
	14	6.231	6.528	4.912
	15	46.017	47.852	33.881
	Sum	53.355	55.634	40.291
Naphtenes	9	1.262	1.273	1.563
	10	0.250	0.245	0.278
	12	0.082	0.080	0.076
	Sum	1.594	1.598	1.918
Olefins	5	0.153	0.185	0.341
	6	1.545	1.792	3.090
	7	0.085	0.099	0.136
	9	0.151	0.165	0.187
	12	0.272	0.286	0.252
	13	0.229	0.239	0.196
	4	0.748	0.775	0.596
	16	1.209	1.237	0.842
	Sum	4.391	4.777	5.641
Paraffins	9	0.164	0.182	0.200
	15	0.074	0.077	0.055
	16	2.438	2.527	1.684
	Sum	2.676	2.785	1.938
Unknowns	6	0.246	0.296	0.446
	7	0.202	0.234	0.313
	10	0.416	0.453	0.457
	11	1.463	1.571	1.464
	12	1.100	1.174	1.010
	13	2.845	3.006	2.414
	Sum	6.271	6.733	6.103
Total		100	100	100

Conclusions

Catalytic cracking of cracked PFO was carried out in a semi-batch reactor. Two different kinds of catalyst, ZSM-5, and MCM-41, were used. Also, two modification methods, ion exchange and impregnation with Fe and Ti were studied.

The relative crystallinity of MCM-41 catalysts was calculated using the XRD pattern of the origin and modified form of MCM-41 catalysts. Relative crystallinity of H-MCM-41, Fe/Al-MCM-41, and Ti/H-MCM-41 are 96.4%, 85.7%, and 81.4%, respectively. It means, by impregnating the MCM-41 zeolite, the relative crystallinity of samples falls under 20%, so the structure of the zeolite during the modification is unchanged and the modified samples have high catalytic activity.

Effect of two different modifications, ion exchange and impregnation with Fe and Ti, on the ZSM-5 and MCM-41 base catalyst were studied in the catalytic cracking of cracked PFO. 3%Ti/H-MCM-41 catalyst has the best catalytic activity among all catalysts. Ti/H-MCM-41 has the highest amount of liquid product with the lowest viscosity which means this catalyst is a suitable catalyst for upgrading heavy feedstock such as PFO.

The experimental design was utilized to optimize the liquid and gas product distribution using a five-level central composite design model. Increasing temperature increases liquid yield and viscosity which reduces the quality of the liquid product, as well. So, moderate temperature (between 370-390 °C) is suitable to obtain a high amount of liquid products with high quality. Also, when the temperature is between 370-390 °C, the maximum yield of light olefin of the gas product can be obtained. An increasing catalyst to feed ratio and the loading of Ti slightly decreases the liquid yield, but viscosity reduces widely, so to obtain a high-quality liquid, a High amount of catalyst should be used in the reaction. Also, when the catalyst to feed ratio is more than 0.085 and the loading of Ti is between 0.75-2.75 %, the maximum yield of light olefin of the gas product can be obtained.

The desirability factor is utilized to obtain the optimum condition to maximize the liquid yield and total olefin of the gas product and to minimize the viscosity. The optimum condition of temperature, catalyst to feed ratio, and loading of Ti are between 370-390 °C, 0.085-0.1, and 1-3 %, respectively.

The best catalyst is 2.5%Ti/H-MCM-41 in reaction tests. The liquid product of optimum condition was analyzed. 26 wt. % of the liquid was in the range of gasoline (C_5-C_{10}) and the rest of the liquid product was in the range of light gasoil (C_{11}-C_{16}). A large amount of liquid product is iso-paraffins and aromatic compounds are very suitable to use as liquid fuels. At 37.8 °C, the viscosity of the feed is 5.1255 mm^2/s which is out of the suitable viscosity of light gas oil i.e. 3-5 mm^2/s range. The viscosity of the liquid product in optimum condition is 3.1686 mm^2/s at 37.8 °C, so the viscosity reduction is a key proof for producing high-quality fuel in the range of gasoline and light gas oil.

List of Symbols

A	Temperature of reaction(°C)
B	Catalyst to feed ratio (-)
C	Loading of metal (wt. %)

List of Greek Letters

Θ	Angle(°)

References

[1] Zhichang LI, Xianghai ME, Chunming XU, Jinsen GA. Secondary cracking of gasoline and diesel from heavy oil catalytic pyrolysis. Chinese Journal of Chemical Engineering. 2007 Jun 1;15(3):309-14.

[2] Meng X, Xu C, Gao J, Zhang Q. Effect of catalyst to oil weight ratio on gaseous product distribution during heavy oil catalytic pyrolysis. Chemical Engineering and Processing: Process Intensification. 2004 Aug 1;43(8):965-70.
[3] Basily IK, Souaya ER, Ibraheem NN. Gas-liquid chromatographic determination of the gaseous products of the two-stage pyrolysis of heavy oils. Microchemical Journal. 1988 Dec 1;38(3):283-94.
[4] Gao X, Qin Z, Wang B, Zhao X, Li J, Zhao H, Liu H, Shen B. High silica REHY zeolite with low rare earth loading as high-performance catalyst for heavy oil conversion. Applied Catalysis A: General. 2012 Jan 31;413:254-60
[5] Zhang Y, Yu D, Li W, Gao S, Xu G, Zhou H, Chen J. Fundamental study of cracking gasification process for comprehensive utilization of vacuum residue. Applied Energy. 2013 Dec 1;112:1318-25.
[6] Zhang Y, Yu D, Li W, Gao S, Xu G. Bifunctional catalyst for petroleum residue cracking gasification. Fuel. 2014 Jan 30;117:1196-203.
[7] Ding F, Ng SH, Xu C, Yui S. Reduction of light cycle oil in catalytic cracking of bitumen-derived crude HGOs through catalyst selection. Fuel Processing Technology. 2007 Sep 1;88(9):833-45.
[8] Li X, Li C, Zhang J, Yang C, Shan H. Effects of Temperature and Catalyst to Oil Weight Ratio on the Catalytic Conversion of Heavy Oil to Propylene Using ZSM-5 and USY Catalysts. Journal of Natural Gas Chemistry. 2007 March 1;16(1):92-9.
[9] Vuong GT, Hoang VT, Nguyen DT, Do TO. Synthesis of nanozeolites and nanozeolite-based FCC catalysts, and their catalytic activity in gas oil cracking reaction. Applied Catalysis A: General. 2010 Jul 15;382(2):231-9.
[10] Ishihara A, Kimura K, Owaki A, Inui K, Hashimoto T, Nasu H. Catalytic cracking of VGO by hierarchical ZSM-5 zeolite containing mesoporous silica–aluminas using a Curie point pyrolyzer. Catalysis Communications. 2012 Nov 5;28:163-7.
[11] Aguado J, Serrano DP, Escola JM, Peral A. Catalytic cracking of polyethylene over zeolite mordenite with enhanced textural properties. Journal of Analytical and Applied Pyrolysis. 2009 May 1;85(1–2):352-8.
[12] Angyal A, Miskolczi N, Bartha L, Tungler A, Nagy L, Vida L, Nagy G. Production of steam cracking feedstocks by mild cracking of plastic wastes. Fuel Processing Technology. 2010 Nov 1;91(11):1717-24.
[13] Singh J, Kumar MM, Saxena AK, Kumar S. Studies on thermal cracking behavior of residual feedstocks in a batch reactor. Chemical Engineering Science. 2004 Nov 1;59(21):4505-15.
[14] Asgharzadeh Shishavan R, Ghashghaee M, Karimzadeh R. Investigation of kinetics and cracked oil structural changes in thermal cracking of Iranian vacuum residues. Fuel Processing Technology. 2011 Dec 1;92(12):2226-34.
[15] Serrano DP, Aguado J, Escola JM, Rodriguez JM, Peral A. Catalytic properties in polyolefin cracking of hierarchical nanocrystalline HZSM-5 samples prepared according to different strategies. Journal of Catalysis. 2010 Nov 19;276(1):152-60.
[16] Wang L, Wang Y, Hao J, Liu G, Ma X, Hu S. Synthesis of HZSM-5 coatings on the inner surface of stainless steel tubes and their catalytic performance in n-dodecane cracking. Applied Catalysis A: General. 2013 Jul 10;462–463:271-7.
[17] Al-Shammari AA, Ali SA, Al-Yassir N, Aitani AM, Ogunronbi KE, Al-Majnouni KA, et al. Catalytic cracking of heavy naphtha-range hydrocarbons over different zeolites structures. Fuel Processing Technology. 2014 Jun 1;122:12-22.
[18] Jeon SG, Kwak NS, Rho NS, Ko CH, Na JG, Yi KB, Park SB. Catalytic pyrolysis of Athabasca bitumen in H_2 atmosphere using microwave irradiation. Chemical Engineering Research and Design. 2012 Sep 1;90(9):1292-6.
[19] Luik H, Luik L, Johannes I, Tiikma L, Vink N, Palu V, Bitjukov M, Tamvelius H, Krasulina J, Kruusement K, Nechaev I. Upgrading of Estonian shale oil heavy residuum bituminous fraction by catalytic hydroconversion. Fuel Processing Technology. 2014 Aug 1;124:115-22.
[20] Han SY, Lee CW, Kim JR, Han NS, Choi WC, Shin CH, Park YK. Selective Formation of Light Olefins by the Cracking of Heavy Naphtha over Acid Catalysts. Studies in Surface Science and Catalysis. 2004;153:157-60.

[21] Fesharaki MJ, Ghashghaee M, Karimzadeh R. Comparison of four nanoporous catalysts in thermocatalytic upgrading of vacuum residue. Journal of Analytical and Applied Pyrolysis. 2013 Jul 1;102:97-102.
[22] Basily IK, Ahmed E, Ibraheam NN. Upgrading heavy ends into marketable products. New concepts and new catalysts for two-stage catalytic pyrolysis. Journal of Analytical and Applied Pyrolysis. 1995 Apr 1;32:221-32.
[23] Ali MA, Tatsumi T, Masuda T. Development of heavy oil hydrocracking catalysts using amorphous silica-alumina and zeolites as catalyst supports. Applied Catalysis A: General. 2002 Jul 10;233(1–2):77-90.
[24] Gao X, Tang Z, Zhang H, Ji D, Lu G, Wang Z, Tan Z. Influence of particle size of ZSM-5 on the yield of propylene in fluid catalytic cracking reaction. Journal of Molecular Catalysis A: Chemical. 2010 Jun 15;325(1–2):36-9.
[25] Zhao L, Gao J, Xu C, Shen B. Alkali-treatment of ZSM-5 zeolites with different SiO2/Al2O3 ratios and light olefin production by heavy oil cracking. Fuel Processing Technology. 2011 Mar 1;92(3):414-20.
[26] Coriolano ACF, Silva CGC, Costa MJF, Pergher SBC, Caldeira VPS, Araujo AS. Development of HZSM-5/AlMCM-41 hybrid micro–mesoporous material and application for pyrolysis of vacuum gasoil. Microporous and Mesoporous Materials. 2013 May 15;172:206-12.
[27] Chen W, Han D, Sun X, Li C. Studies on the preliminary cracking of heavy oils: Contributions of various factors. Fuel. 2013 Apr 1;106:498-504.
[28] Rosenholm JB, Rahiala H, Puputti J, Stathopoulos V, Pomonis P, Beurroies I, et al. Characterization of Al- and Ti-modified MCM-41 using adsorption techniques. Colloids and Surfaces A: Physicochemical and Engineering Aspects. 2004 Dec 1;250(1–3):289-306.
[29] Schacht P, Noreña-Franco L, Ancheyta J, Ramírez S, Hernández-Pérez I, García LA. Characterization of hydrothermally treated MCM-41 and Ti-MCM-41 molecular sieves. Catalysis Today. 2004 Nov 24;98(1–2):115-21.
[30] Hao K, Shen B, Wang Y, Ren J. Influence of combined alkaline treatment and Fe–Ti-loading modification on ZSM-5 zeolite and its catalytic performance in light olefin production. Journal of Industrial and Engineering Chemistry. 2012 Sep 25;18(5):1736-40.
[31] Wang S, Shi Y, Ma X. Microwave synthesis, characterization and transesterification activities of Ti-MCM-41. Microporous and Mesoporous Materials. 2012 Jul 1;156:22-8.
[32] Trong On D, Nguyen SV, Hulea V, Dumitriu E, Kaliaguine S. Mono- and bifunctional MFI, BEA and MCM-41 titanium-molecular sieves. Part 1. Synthesis and characterization. Microporous and Mesoporous Materials. 2003 Jan 16;57(2):169-80.
[33] Lin K, Pescarmona PP, Vandepitte H, Liang D, Van Tendeloo G, Jacobs PA. Synthesis and catalytic activity of Ti-MCM-41 nanoparticles with highly active titanium sites. Journal of Catalysis. 2008 Feb 15;254(1):64-70.
[34] Sedighi M, Keyvanloo K, Towfighi J. Kinetic study of steam catalytic cracking of naphtha on a Fe/ZSM-5 catalyst. Fuel. 2013 Jul 1;109:432-8.
[35] Varzaneh AZ, Kootenaei AHS, Towfighi J, Mohamadalizadeh A. Optimization and deactivation study of Fe–Ce/HZSM-5 catalyst in steam catalytic cracking of mixed ethanol/naphtha feed. Journal of Analytical and Applied Pyrolysis. 2013 Jul 1;102:144-53.
[36] Taghipour N, Towfighi J, Mohamadalizadeh A, Shirazi L, Sheibani S. The effect of key factors on thermal catalytic cracking of naphtha over Ce–La/SAPO-34 catalyst by statistical design of experiments. Journal of Analytical and Applied Pyrolysis. 2013 Jan 1;99:184-90.
[37] Wei Y, Liu Z, Wang G, Qi Y, Xu L, Xie P, He Y. Production of light olefins and aromatic hydrocarbons through catalytic cracking of naphtha at lowered temperature. Studies in Surface Science and Catalysis. 2005 Jan 1;158:1223-30.